Int. J. Solids Structures, 1975, Vol. 11, pp. 555–568. Pergamon Press. Printed in Great Britain

STRESS FINITE-ELEMENT MODELS WITH INDEPENDENT STRAINS

JOHN P. WOLF

Electro-Watt Engineering Services, Zurich, Switzerland

(*Received* 20 *May* 1974; *revised* 25 *July* 1974)

Abstract—Stress finite-element models with an independent expansion for strain are developed. By adding the constitutive law, which is satisfied on the average only, as a condition of constraint to the functional, the variational principle on which they are based is derived. A model which is stiffer can thus be constructed. As the equilibrium models lead to results which are too flexible, an independent assumption for strain should in many cases improve the accuracy. The strains can easily be eliminated on an element basis. A quadrilateral hybrid stress model with an independent assumption of strain is developed and tested on the level of an element and of the structural system.

INTRODUCTION

In a finite-element analysis of an elastic continuum using stress models, of which the equilibrium model of Fraeijs de Veubeke [1] and the hybrid model pioneered by Pian [2, 3] are best known, the constitutive law is regarded as a subsidiary condition. The strain energy is thus expressed as a function of the assumed stress expansion only. By not assuming the constitutive law to be satisfied *a priori* and by introducing it as a condition of constraint in the functional, on which the finite-element formulation is based, an independent expansion for strain in addition to that of stress can be selected. The strain energy is a function of both. A model which is stiffer can be derived, as is shown in this article. The stress model with an independent assumption for strain is thus bounded from above by the corresponding element of which the material law is satisfied exactly. A lower bound to the energy can be verified only numerically. As the equilibrium models and, for certain problems, some hybrid models lead to results which are too flexible for prescribed exterior loads, an independent assumption for the strains should, in many cases, improve the accuracy. As the strains can easily be eliminated on an element basis, the formulation does not really become more complicated.

In the following section, the variational principle and the finite-element formulation are summarized. A quadrilateral hybrid stress model with an independent assumption of strain for a moderately thick plate element in bending is developed. Extensive numerical experimentation on the level of an element and of the structural system is performed. Details can be found in Ref. [4], were, in addition, more general stress models are examined.

VARIATIONAL PRINCIPLE

By introducing the strain-displacement relations and the geometric boundary conditions into the principle of minimum potential energy, and integrating by parts, the three-field Hu-Washizu principle [5]

$$\pi(\sigma_{ij}, \epsilon_{ij}, u_i) = \int_V \left(\frac{1}{2} \cdot \epsilon_{ij} \cdot E_{ijkl} \cdot \epsilon_{kl} - \epsilon_{ij} \cdot \sigma_{ij}\right) \cdot \mathrm{d}V - \int_V (\sigma_{ij,j} + \bar{F}_i) \cdot u_i \cdot \mathrm{d}V + \int_{S_\sigma} (T_i - \bar{T}_i) \cdot u_i \cdot \mathrm{d}S + \int_{Su} T_i \cdot \bar{u}_i \cdot \mathrm{d}S \qquad (1)$$

is derived, where V is the volume, S_σ and S_u the portions of the boundary where the surface tractions $\bar{T}_i$ and displacements $\bar{u}_i$, respectively, are prescribed. ϵ_{ij} represents the strain tensor, E_{ijkl} the elastic-stiffness tensor and σ_{ij} the stress tensor. $\bar{F}_i$ are the prescribed body forces, u_i the displacements and $T_i = \sigma_{ij} \cdot \nu_j$ the surface tractions, ν_j being the components of the unit vector normal to the boundary.

For a finite-element analysis, it is convenient to generalize the stationary principle as follows:

$$\Pi(\sigma_{ij}, \epsilon_{ij}, u_i, \tilde{u}_i) = \sum_n \left\{ \int_{V_n} \left(\frac{1}{2} \cdot \epsilon_{ij} \cdot E_{ijkl} \cdot \epsilon_{kl} - \epsilon_{ij} \cdot \sigma_{ij} \right) \cdot \mathrm{d}V \right.$$
$$\left. - \int_{V_n} (\sigma_{ij,j} + \bar{F}_i) \cdot u_i \cdot \mathrm{d}V - \int_{S_{\sigma_n}} \bar{T}_i \cdot \tilde{u} \cdot \mathrm{d}S + \int_{\partial V_n} T_i \cdot \tilde{u}_i \cdot \mathrm{d}S \right\} \tag{2}$$

where n is the number of finite elements, $\tilde{u}_i$ are the independent boundary displacements common to two adjacent elements and on S_{u_n}, $\tilde{u}_i = \bar{u}_i$ is assumed. If the constitutive law is satisfied *a priori*,

$$\epsilon_{ij} = C_{ijkl} \cdot \sigma_{kl} \tag{3}$$

C_{ijkl} representing the elastic compliance tensor, the first integral of the functional equation (2) is transformed as

$$\int_{V_n} \left(\frac{1}{2} \cdot \epsilon_{ij} \cdot E_{ijkl} \cdot \epsilon_{kl} - \epsilon_{ij} \cdot \sigma_{ij} \right) \cdot \mathrm{d}V \rightarrow \int_{V_n} \frac{1}{2} \cdot \sigma_{ij} \cdot C_{ijkl} \cdot \sigma_{kl} \cdot \mathrm{d}V \tag{4}$$

the other integrals not being affected. In this form, the stationary variational principle $\Pi(\sigma_{ij}, u_i, \tilde{u}_i)$ forms the basis of many stress models, e.g. the equilibrium model [1, 3], the hybrid model [2, 3], the alternate hybrid and extended hybrid models [4, 6] and various generalizations [4].

FINITE-ELEMENT FORMULATION

As an independent assumption of strain affects only the term representing the strain-energy of the variational principle (equation 2) and the finite-element formulation of conventional stress models is rather well documented [6, 7], the discussion will be restricted to the modifications expressed by equation (4). Independent assumptions are made for the stresses σ_{ij} and strains ϵ_{ij} of each element

$$\{\sigma\} = [P] \cdot \{\beta\} \tag{5}$$
$$\{\epsilon\} = [M] \cdot \{\gamma\} \tag{6}$$

where $\{\beta\}$, $\{\gamma\}$ are columns of undetermined parameters and $[P]$, $[M]$ are sets of functions (polynomials). Substituting equations (5, 6) into the first integral of equation (2), the strain energy is formulated as

$$\sum_n \left\{ + \frac{1}{2} \cdot \{\gamma\}^t \cdot [H_{\epsilon\epsilon}] \cdot \{\gamma\} - \{\gamma\}^t \cdot [H_{\epsilon\sigma}] \cdot \{\beta\} \right\} \tag{7}$$

whereby

$$[H_{\epsilon\epsilon}] = \int_{V_n} [M]^t \cdot [E] \cdot [M] \cdot \mathrm{d}V \tag{8}$$

$$[H_{\epsilon\sigma}] = \int_{V_n} [M]^t \cdot [P] \cdot \mathrm{d}V. \tag{9}$$

Setting the first variation of the functional (equation 7) with respect to $\{\gamma\}$, which can be varied independently for each element, equal to zero, leads to the discrete form of the constitutive law

$$[H_{\epsilon\epsilon}] \cdot \{\gamma\} - [H_{\epsilon\sigma}] \cdot \{\beta\} = 0. \tag{10}$$

After eliminating $\{\gamma\}$ from equation (10) and defining the flexibility matrix $[H_{\sigma\sigma}]$ as

$$[H_{\sigma\sigma}] = [H_{\epsilon\sigma}]^t \cdot [H_{\epsilon\epsilon}]^{-1} \cdot [H_{\epsilon\sigma}] \tag{11}$$

the strain energy, equation (7) is written as

$$\sum_n -\frac{1}{2} \cdot \{\beta\}^t \cdot [H_{\sigma\sigma}] \cdot \{\beta\}. \tag{12}$$

$[H_{\epsilon\epsilon}]$ and $[H_{\sigma\sigma}]$ are positive definite matrices, as the material law $[E]$ exhibits the same property. In the conventional stress models, where the constitutive law is subsidiary, the strain energy (right-hand side of equation 4) is formulated as in equation (12), with $[H_{\sigma\sigma}]$ being replaced by $[H]$

$$[H] = \int_{V_n} [P]^t \cdot [C] \cdot [P] \cdot dV. \tag{13}$$

It should be noted that this static condensation process, involving $\{\gamma\}$, is analogous to the procedure used by Willam[8]. The constitutive law can be used to eliminate the stresses and not the strains, as is normally done, from the general Hu-Washizu principle (equation 1). This leads to the Hellinger-Reissner principle involving u_i and ϵ_{ij} as free variables. Willam eliminates ϵ_{ij} on an element basis, for which no continuity is imposed. The analogue of equation (11) is a stiffness matrix. Many of Willam's conclusions appropriately modified also apply to the models discussed in this article although different laws are involved, vis. in Willam's mixed model with independent strains, the strain-displacement equations and in the generalized stress models, the constitutive law (equation 3).

As the functional, equation (2) does not involve derivatives of the strains, the continuity of the strain field need not be imposed for convergence. The constant-strain criterion (also called completeness condition) is obviously satisfied if constant terms are present in the $\{\epsilon\}$-expansion (equation 6). This allows the constitutive law to be satisfied exactly for an infinitesimal element. In addition, it follows from equations (10, 11) that the number of γ's must be larger or the same as the number of β's. If not, the matrix $[H_{\sigma\sigma}]$ (equation 11) is singular.

The following possibilities of selecting the expansions for $\{\sigma\}$ and $\{\epsilon\}$ exist:

(a) If $\{\sigma\}$ and $\{\epsilon\}$ are approximated by (complete) polynomials of the same order, the constitutive law will be satisfied for an element of finite length. The two matrices $[H_{\sigma\sigma}]$ and $[H]$ are identical.

(b) If $\{\epsilon\}$ is approximated by a polynomial of higher order than that of $\{\sigma\}$, again identical discretization matrices $[H_{\sigma\sigma}]$ and $[H]$ are derived. The coefficients of the higher order terms of $\{\epsilon\}$, which do not exist in $\{\sigma\}$, will be zero. This is the best way, in the sense of energy considerations, of satisfying the discrete form of the constitutive law, equation (10). This would not be the case if continuity requirements were imposed on $\{\epsilon\}$.

(c) If certain components of $\{\epsilon\}$ are approximated by polynomials of lower order than or by incomplete polynomials of the same order as that of $\{\sigma\}$, the two matrices $[H_{\sigma\sigma}]$ and $[H]$ will

differ. As described above, a non-singular $[H_{\sigma\sigma}]$-matrix has to be derived. As certain components of $\{\epsilon\}$ have to vary with a polynomial of lower degree than the strains calculated from $\{\sigma\}$ using the constitutive law, the element is stiffer. The inequality

$$[H_{\sigma\sigma}] \leq [H] \tag{14}$$

holds. As the inverse of $[H_{\sigma\sigma}]$ or of $[H]$ is used to calculate the stiffness matrix $[K]$, each term of the $[K]$-matrix based on a strain assumption is larger than or equal to the corresponding term of the $[K]$-matrix which assumes the constitutive law satisfied *a priori*. Willam [8] proved rigorously for Poisson's ratio $\nu = 0$, using the inequality of Schwartz, that his mixed model, with an independent assumption for $\{\epsilon\}$, is more flexible than the corresponding displacement model. The same proof could be used here. A simple example is given for illustration in Ref. [4].

QUADRILATERAL MODERATELY THICK PLATE-BENDING ELEMENT

To show how the different matrices are constructed, a hybrid stress model for a quadrilateral moderately thick plate-bending element is derived. It is then generalized by selecting an independent expansion for the strains. At first, the model for a square element is constructed. Using the isoparametric mapping procedure the square element can be distorted into a general quadrilateral element (Fig. 1).

Hybrid stress models for a plate in bending, including the effect of transverse-shear deformability, were discussed, among others, by Mau *et al.* [9, 10]. In Ref. [10], the behavior of quadrilateral elements is compared, either derived directly or from triangles, either based on linear or complete or incomplete quadratic expansions for the stresses and on either linear or (partially) quadratic polynomials for the displacements along the inter-element boundary. The evaluation, which was performed for thick and thin plates, showed that the quadrilateral element based on a linear expansion for the stresses and the inter-element displacements, converged the most rapidly. The same expansions are used here.

The isotropic element (modulus of elasticity E, Poisson's ratio ν) with the side length $2a$ and thickness h is shown on the left-hand side of Fig. 1.

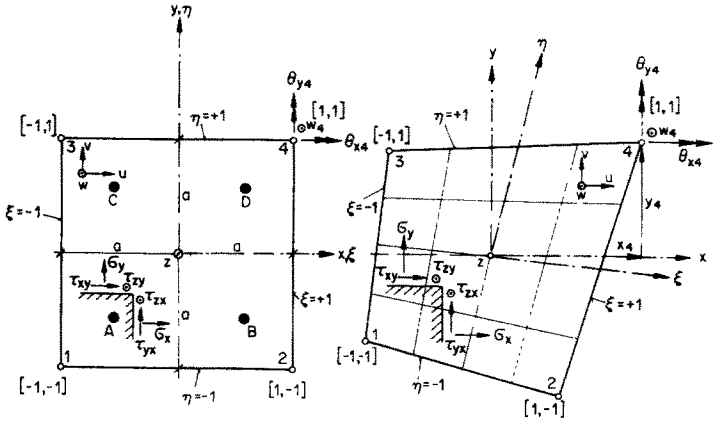

Fig. 1. Square parent element and distorted quadrilateral element.

The following expansions are selected for the stresses, which satisfy the homogeneous equations of equilibrium for a three-dimensional body:

$$\sigma_x(x, y, z) = \beta_1 \cdot \frac{z}{\frac{h}{2}} + \beta_2 \cdot \frac{x}{a} \cdot \frac{z}{\frac{h}{2}} + \beta_3 \cdot \frac{y}{a} \cdot \frac{z}{\frac{h}{2}} \tag{15a}$$

$$\sigma_y(x, y, z) = \beta_4 \cdot \frac{z}{\frac{h}{2}} + \beta_5 \cdot \frac{x}{a} \cdot \frac{z}{\frac{h}{2}} + \beta_6 \cdot \frac{y}{a} \cdot \frac{z}{\frac{h}{2}} \tag{15b}$$

$$\tau_{xy}(x, y, z) = \beta_7 \cdot \frac{z}{\frac{h}{2}} + \beta_8 \cdot \frac{x}{a} \cdot \frac{z}{\frac{h}{2}} + \beta_9 \cdot \frac{y}{a} \cdot \frac{z}{\frac{h}{2}} \tag{15c}$$

$$\tau_{xz}(z) = \beta_2 \cdot \left(\frac{h}{4a} - \frac{z^2}{a \cdot h}\right) + \beta_9 \cdot \left(\frac{h}{4a} - \frac{z^2}{a \cdot h}\right) \tag{15d}$$

$$\tau_{yz}(z) = \beta_6 \cdot \left(\frac{h}{4a} - \frac{z^2}{a \cdot h}\right) + \beta_8 \cdot \left(\frac{h}{4a} - \frac{z^2}{a \cdot h}\right) \tag{15e}$$

$$\sigma_z = 0. \tag{15f}$$

The flexibility matrix $[H]$ (equation 13) is calculated as follows:

$$\{\beta\}' \cdot [H] \cdot \{\beta\} = \frac{1}{E} \cdot \int_V \{\sigma_x^2 + \sigma_y^2 - 2 \cdot \nu \cdot \sigma_x \cdot \sigma_y + 2(1+\nu)\tau_{xy}^2 + 2 \cdot (1+\nu) \cdot \tau_{xz}^2 + 2 \cdot (1+\nu) \cdot \tau_{yz}^2\} \, dz \cdot dA. \tag{16}$$

For a plate with transverse-shear deformability, the rotations and the lateral displacement have to be assumed independently. Linear expansions $\tilde{u}_i$ along the boundary are selected. If a displacement function u_i over the element can be constructed which is compatible with the assumed boundary displacement $\tilde{u}_i$, the integrations which have to be performed along the boundary to determine the so-called $[G]$-matrix[3, 9, 10] can be replaced by an integration over the volume of the element. Bi-linear expansions in the skew coordinate system ξ, η (see Fig. 1) are selected. The values of ξ, η on the faces of the elements are ± 1. Coordinates ξ_i, η_i of the four corner points are introduced, which are equal to the values of ξ, η of the faces meeting at the corners. The following displacement expansion is formulated:

$$u(\xi, \eta, \zeta) = \frac{1}{4} \cdot z \cdot \sum_{i=1}^{4} (1 + \xi_i \cdot \xi) \cdot (1 + \eta_i \cdot \eta) \cdot \theta_{yi} \tag{17a}$$

$$v(\xi, \eta, \zeta) = -\frac{1}{4} \cdot z \cdot \sum_{i=1}^{4} (1 + \xi_i \cdot \xi) \cdot (1 + \eta_i \cdot \eta) \cdot \theta_{xi} \tag{17b}$$

$$w(\xi, \eta) = \frac{1}{4} \cdot \sum_{i=1}^{4} (1 + \xi_i \cdot \xi) \cdot (1 + \eta_i \cdot \eta) \cdot w_i. \tag{17c}$$

The stiffness matrix $[K]$ and the stress-displacement matrix of the hybrid stress model can thus be calculated.

The following assumptions for the strains are chosen

$$\epsilon_x(x, y, z) = \gamma_1 \cdot \frac{z}{\frac{h}{2}} + \gamma_2 \cdot \frac{x}{a} \cdot \frac{z}{\frac{h}{2}} + \gamma_3 \cdot \frac{y}{a} \cdot \frac{z}{\frac{h}{2}} \tag{18a}$$

$$\epsilon_y(x, y, z) = \gamma_4 \cdot \frac{z}{\frac{h}{2}} + \gamma_5 \cdot \frac{x}{a} \cdot \frac{z}{\frac{h}{2}} + \gamma_6 \cdot \frac{y}{a} \cdot \frac{z}{\frac{h}{2}} \tag{18b}$$

$$\gamma_{xy}(z) = \gamma_7 \cdot \frac{z}{\frac{h}{2}} \tag{18c}$$

$$\gamma_{xz}(z) = \gamma_8 \cdot \left\{1 - \left(\frac{z}{\frac{h}{2}}\right)^2\right\} \tag{18d}$$

$$\gamma_{yz}(z) = \gamma_9 \cdot \left\{1 - \left(\frac{z}{\frac{h}{2}}\right)^2\right\} \tag{18e}$$

$$\epsilon_z(z) = \gamma_{10} \cdot \frac{z}{\frac{h}{2}}. \tag{18f}$$

On the upper and lower face, the shear strains γ_{xz}, γ_{yz} (equations 18d, 18e) are zero, the same for the shear stresses τ_{xz}, τ_{yz} (equations 15d, 15e). The expansion lacks invariance, as γ_{xy} (equation 18c) is not a function of x, y. The strain energy of the three-dimensional elastic body, expressed as a function of the strains, defines the $[H_{\epsilon\epsilon}]$-matrix (equation 8).

$$\begin{aligned}\{\gamma\}^t \cdot [H_{\epsilon\epsilon}] \cdot \{\gamma\} = {} & \frac{(1-\nu) \cdot E}{(1-2\nu) \cdot (1+\nu)} \cdot \int_V \left\{\epsilon_x^2 + \epsilon_y^2 + \epsilon_z^2 \right. \\ & \left. + \frac{2\nu}{1-\nu} \cdot \epsilon_x \cdot \epsilon_y + \frac{2\nu}{1-\nu} \cdot \epsilon_x \cdot \epsilon_z + \frac{2\nu}{1-\nu} \cdot \epsilon_y \cdot \epsilon_z \right\} \cdot dz \cdot dA \\ & + \frac{E}{2(1+\nu)} \cdot \int_V (\tau_{xy}^2 + \tau_{xz}^2 + \tau_{yz}^2) \cdot dz \cdot dA. \end{aligned} \tag{19}$$

The $[H_{\epsilon\sigma}]$-matrix (equation 9) follows from

$$\{\gamma\}^t \cdot [H_{\epsilon\sigma}] \cdot \{\beta\} = \int_V (\epsilon_x \cdot \sigma_x + \epsilon_y \cdot \sigma_y + \epsilon_z \cdot \sigma_z + \gamma_{xy} \cdot \tau_{xy} + \gamma_{xz} \cdot \tau_{xz} + \gamma_{yz} \cdot \tau_{yz}) \cdot dz \cdot dA. \tag{20}$$

After calculating the $[H_{\sigma\sigma}]$-matrix (equation 11), the stiffness matrix $[K]$ and the stress-displacement matrix of the generalized hybrid stress model with an independent assumption for strain can easily be determined. For laminated plates [9, 10], the shear stresses τ_{xz}, τ_{yz} and shear strains γ_{xz}, γ_{yz} are obviously not zero on the top and bottom faces of the individual layers (excluding the top and bottom face of the plate). For the bending portion of such a layer, the stress assumption equation (21) together with equations (15a, b, c, f) and the strain expansion equation (22), together with equations (18a, b, c, f) are used.

$$\tau_{xz}(z) = \beta_{10} - (\beta_2 + \beta_9) \cdot \frac{z^2}{a \,.\, h} \tag{21a}$$

$$\tau_{yz}(z) = \beta_{11} - (\beta_6 + \beta_8) \cdot \frac{z^2}{a \,.\, h} \tag{21b}$$

$$\gamma_{xz}(z) = \gamma_8 \,.\, \left\{1 - \left(\frac{z}{\frac{h}{2}}\right)^2\right\} + \gamma_{11} \tag{22a}$$

$$\gamma_{yz}(z) = \gamma_9 \,.\, \left\{1 - \left(\frac{z}{\frac{h}{2}}\right)^2\right\} + \gamma_{12}. \tag{22b}$$

Using the isoparametric mapping procedure, the parent element is mapped onto a curvilinear one. The coordinate transformation is established using the same shape functions, as those which represent the unknown displacement functions (equation 17).

$$x = \frac{1}{4} \cdot \sum_{i=1}^{4} (1 + \xi_i \,.\, \xi)(1 + \eta_i \,.\, \eta) \,.\, x_i \tag{23a}$$

$$y = \frac{1}{4} \cdot \sum_{i=1}^{4} (1 + \xi_i \,.\, \xi)(1 + \eta_i \,.\, \eta) \,.\, y_i. \tag{23b}$$

Numerical integration is used.

As pointed out by Pian *et al.*[11], the quadrilateral element has two kinematic displacement modes. The rank of the stiffness matrix $[K]$ is only $12 - 3 - 2 = 7$. For the quadrilateral element, the kinematic displacement modes can be eliminated by adding an $x \,.\, y$-term for σ_x (equation 15a) and for σ_y (equation 15b)[11].

NUMERICAL EXPERIMENTATION

To be able to determine the accuracy on an element basis of the same stress model with and without an independent assumption for the strain, all possible boundary-value problems have to be examined. When Willam[8] compared the displacement model and the associated mixed model, the following procedure was used. The spectrum of eigenvalues of the difference matrix, determined from the stiffness matrices of the two elements to be compared, were calculated. It represents the difference of energy stored in a given element for a discrete number of boundary-value problems.

For illustration, the quadrilateral plate-bending elements are used. The difference matrix is formed by subtracting the stiffness matrix $[K]$ of the model without an assumption for strain from that with an independent expansion. The difference matrix is positive definite, expressing that the model with a strain expansion leads to a lower energy than the model without a strain expansion for all displacement boundary conditions which are contained in the set of eigenvectors. This follows from the fact that a suitable chosen strain assumption makes the model stiffer (equation 14). As both elements possess three rigid-body modes, three constant-strain conditions and two kinematic displacement modes, $12 - 3 - 3 - 2 = 4$ positive eigenvalues would be expected. Actually, only two are distinct from zero. In Table 1, the eigenvalues of the difference matrix are listed for different shapes (square element, rhombus element with $\alpha = 30°$, $a = 10$), for different thicknesses ($(h/2a) = 0{\cdot}01$, $(h/2a) = 0{\cdot}125$) and for

Table 1. Eigenvalues and one eigenvector of difference matrix of stiffness matrices with and without strain assumption

		Poisson's Ratio ν				
		0	0167	0 333	0 45	0495
Square Plate	$\frac{h}{2a}$ = 001	9 340	8 005	7 004	6 440	6.246
	$\frac{h}{2a}$ = 0125	111 400	94 812	82 093	74 659	72 009
Rhombus Plate	$\frac{h}{2a}$ = 001	4 345 5 568	3 722 4 772	3253 4175	2 988 3 838	2 897 3 722
	$\frac{h}{2a}$ = 0125	33 833 61.331	27 573 52 849	22 634 46.717	19 708 43 510	18 673 42 500

w_1	3 087 10^{-2}
θ_{x1}	4 032 10^{-1}
θ_{y1}	-8 452 10^{-3}
w_2	5 922 10^{-2}
θ_{x2}	4 977 10^{-1}
θ_{y2}	2 919 10^{-1}
w_3	-5 922 10^{-2}
θ_{x3}	4 977 10^{-1}
θ_{y3}	2 919 10^{-1}
w_4	-3 087 10^{-2}
θ_{x4}	4 032 10^{-1}
θ_{y4}	-8 452 10^{-3}

various Poisson ratio's ($\nu = 0$, 0·167, 0·333, 0·45, 0·495). The two eigenvalues are equal for the square element. The largest eigenvalue of the difference matrix provides a measure of the largest difference in energy. It also isolates the critical boundary-value problem. For the square element ($(h/2a) = (1/100)$, $\nu = 0$), the corresponding eigenvector is listed in Table 1. The largest eigenvalue diminishes with increasing ν. The same happens with the arithmetic mean and with the difference of the eigenvalues for the rhombus, indicating that the difference in energies for different boundary-value problems becomes smaller.

On the structural-systems level, simply supported thin ($(h/l) = 0{\cdot}01$) and thick plates ($(h/l) = 0{\cdot}125$) with $\nu = 0{\cdot}3$ are analyzed for a distributed load p and a central concentrated load P. Analytical solutions have been determined by Timoshenko for the thin plate[12] and by Reissner for the moderately thick plate under a distributed load[13]. Kirchhoff-type boundary conditions are enforced.

$$w = 0 \tag{24a}$$

$$\phi_s = 0. \tag{24b}$$

Meshes 1×1, 2×2, 4×4 and 8×8 for a quarter of the plate are selected, leading to 12, 27, 75 and 243 unknowns, respectively (before enforcing boundary conditions). All four models are used. The symbol σ_l^u is attached to the hybrid model enforcing zero transverse-shear stress τ_{xz}, τ_{yz} on the upper and lower face (equation 15), the symbol $\sigma_l^u\,\epsilon_l^u$, when in addition strains are assumed with zero transverse shear strain γ_{xz}, γ_{yz} on the upper and lower face (equation 18). The symbols σ and $\sigma\epsilon$ are used, when the stress assumption (equations 15a, b, c, f, 21) and in addition the strain assumptions (equations 18a, b, c, f, 22), respectively, do not satisfy any special "boundary conditions" on the upper and lower face.

Some results of the various finite-element calculations are shown in Table 2. The energy π is determined by summing the product of the concentrated vertical load and the displacement in each node over the whole plate. All models converge. Choosing an independent expansion for the strains does indeed make the model stiffer. For the distributed load, the vertical displacement for the thin and thick plates converges from above for the model σ_l^u and from below for $\sigma_l^u\,\epsilon_l^u$. However, for both models, the energy converges from below. For the concentrated load, the energy (and thus the displacement) converges from different sides for σ_l^u and for $\sigma_l^u\,\epsilon_l^u$. The

Table 2. Simply supported plate calculated with different stress and strain assumptions

			Distributed Load p									
			Thin Plate ($\frac{h}{l}$ = 0.01)					Thick Plate ($\frac{h}{l}$ = 0.125)				
			1 x 1	2 x 2	4 x 4	8 x 8	analytical	1 x 1	2 x 2	4 x 4	8 x 8	analytical
Energy π	σ_l^u	$10^{-3}\cdot \frac{p^2 l^6}{D}$	1.070	1.520	1.656	1.691	1.702	1.209	1.671	1.811	1.848	1.836
	σ_l^u ε_l^u		0.353	1.293	1.596	1.676		0.492	1.444	1.751	1.832	
	σ		0.798	1.456	1.639	1.686		0.915	1.584	1.771	1.818	
	σ ε		0.002	0.048	0.587	1.518		0.282	1.345	1.750	1.816	
Vertical Displacement w (Centre)	σ_l^u	$10^{-3}\cdot \frac{p l^4}{D}$	4.280	4.109	4.074	4.066	4.062	4.834	4.479	4.409	4.396	4.357
	σ_l^u ε_l^u		1.411	3.532	3.937	4.032		1.966	3.898	4.273	4.362	
	σ		3.192	3.971	4.043	4.058		3.660	4.285	4.326	4.335	
	σ ε		0.008	0.130	1.461	3.660		1.127	3.636	4.276	4.330	
Bending Moment m_x (Centre)	σ_l^u	$10^{-2}\cdot p l^2$	4.16	4.62	4.87	4.81	4.79	4.16	4.62	4.87	4.81	4.79
	σ_l^u ε_l^u		1.39	4.18	4.55	4.73		1.39	4.20	4.55	4.73	
	σ		3.13	4.61	4.79	4.79		3.11	4.60	4.76	4.77	
	σ ε		0.00	0.14	1.70	4.30		0.44	3.73	4.56	4.74	
Shear Force q_x (Mid - Boundary)	σ_l^u	$10^{-1}\cdot p l$	1.25	2.27	2.79	3.07	3.38	1.25	2.80	2.79	3.07	3.38
	σ_l^u ε_l^u		1.25	2.24	2.78	3.07		1.25	2.26	2.78	3.07	
	σ		1.25	2.29	2.80	3.08		1.25	2.29	2.80	3.08	
	σ ε		1.25	2.29	2.80	3.08		1.25	2.29	2.80	3.08	

			Concentrated Load P Thin Plate ($\frac{h}{l}$ = 0.01)				
			1 x 1	2 x 2	4 x 4	8 x 8	analytical
Vertical Displacement w (Centre) ~ Energy π	σ_l^u	$10^{-2}\cdot \frac{P l^2}{D}$	1.711	1.341	1.226	1.184	1.160
	σ_l^u ε_l^u		0.564	1.012	1.128	1.156	
	σ		1.276	1.153	1.156	1.160	
	σ ε		0.003	0.037	0.397	1.023	

model σ_l^u ϵ_l^u does lead to the most accurate results for various quantities. Not enforcing the "boundary conditions" on the upper and lower faces leads to a stiffer element. The disastrous results for coarse meshes of the model $\sigma\epsilon$ are due to numerical round-off errors when inverting the $[H_{\epsilon\epsilon}]$-matrix, which in contrast to the same matrix for the model σ_l^u ϵ_l^u is a function of (h/a). The average pivot in the inversion process for the 1×1 mesh is 10^{-1}, the smallest $0{\cdot}85 \times 10^{-5}$. For the model σ_l^u ϵ_l^u, the corresponding values are 0·36 and 0·28. All calculations are performed in single precision (36 bits). For the 8×8 mesh, the results of the model $\sigma\epsilon$ are good. It is interesting to note that the (constant) q_x is not effected by the ill-conditioning of $[H_{\epsilon\epsilon}]$.

Using the displacement functions over the elements (equation 17) which are compatible with the assumed boundary displacements, the mass matrix can easily be calculated. With the stiffness matrix $[K]$ of the hybrid stress model without and with an independent assumption of strains, a dynamic analysis is based on rigorous variational principles, the modified Hellinger–Reissner principle and the corresponding modified Hu-Washizu principle, respectively.

The natural frequencies ω and the corresponding modes of the square thin cantilever plate of Fig. 2 are calculated ($(h/l) = (1/100)$ Poisson's ratio $\nu = 0{\cdot}3$). No exact solution exists. Meshes 1×1, 2×2 and 4×4 for both models σ_l^u and σ_l^u ϵ_l^u are used, leading to 6, 18 and 60 unknowns, respectively. The consistent mass matrix which is not unique as the stresses satisfy internal equilibrium, is based on equation (17). A lumped mass matrix is also used, which is derived by

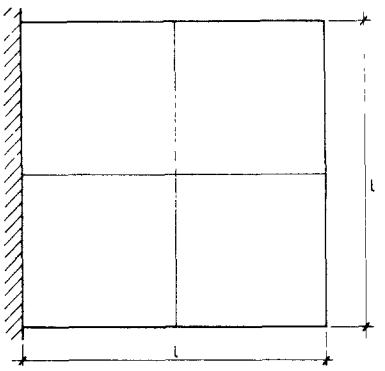

Fig. 2. Square cantilever plate with typical 2 × 2 mesh.

assuming that the displacements within the tributary region of a particular node are identical to the displacements of the node. For comparison, the results of Geradin[14] are used, who calculated the same plate using the displacement model of Fraeijs de Veubeke[15], a quadrilateral element made up of four triangles with cubic displacements and the triangular equilibrium model of Fraeijs de Veubeke *et al.*[16] with linear expansion for the moments. The number of remaining degrees of freedom, including internal displacements, if any, but after enforcement of geometric boundary conditions, is given in Table 3. The natural frequencies of displacement models decrease monotonically to the exact value for finer subdivisions and those of the equilibrium model in this particular case increase.

For each idealization of the structure, the five lower eigenvalues, which are defined by the ratio λ

$$\lambda = \frac{\rho \cdot h \cdot l^4}{D} \cdot \omega^2 \qquad \text{with} \qquad D = \frac{E \cdot h^3}{12 \cdot (1 - \nu^2)} \tag{25}$$

are listed in Table 3. As expected, using the consistent-mass matrix leads to more accurate results than working with the lumped-mass matrix. The eigenvalues determined using the model with an independent assumption of strain σ_i^u ϵ_i^u are larger than those calculated with the model σ_i^u. The lower and upper bounds calculated with a fine mesh of equilibrium and displacement models, respectively, are also specified[14]. In Fig. 3 the second lowest eigenvalue λ_2 is plotted vs the

Table 3. Five lowest eigenvalues using standard hybrid models without σ^u and with $\sigma_i^u \epsilon_i^u$ independent assumption for strain

		Lumped - Mass Matrix			Consistent - Mass Matrix			Bounds Lower (Equil.) Upper (Displ.)
		1x1 Mesh 6 Unkn	2x2 Mesh 18 Unkn	4x4 Mesh 60 Unkn	1x1 Mesh 6 Unkn	2x2 Mesh 18 Unkn	4x4 Mesh 60 Unkn	
λ_1	σ_i^u	1 555	9 796	11 390	6.999	11 647	11 945	12.031
	σ_i^u ϵ_i^u	2 100	10 474	11 652	9 448	12 575	12 227	12.065
λ_2	σ_i^u	6 336	35 261	57 809	9 505	60 006	67 184	72 152
	σ_i^u ϵ_i^u	7 992	57 312	67 938	11 989	99 955	79 040	72 433
λ_3	σ_i^u	130 10^4	69 420	357 986	504 10^4	472 128	510 574	452.02
	σ_i^u ϵ_i^u	134 10^4	102 047	398 091	504 10^4	574 388	575 745	453 62
λ_4	σ_i^u	292 10^4	164 964	463 836	1086 10^4	498 061	779 570	737 76
	σ_i^u ϵ_i^u	298 10^4	189 591	583.643	1116 10^4	647 751	903 198	740 87
λ_5	σ_i^u	1118 10^4	211 234	509 957	1944 10^4	718 096	965 450	954 08
	σ_i^u ϵ_i^u	2334 10^7	340.254	713 306	419 5·10^7	1128 747	1215 586	960 41

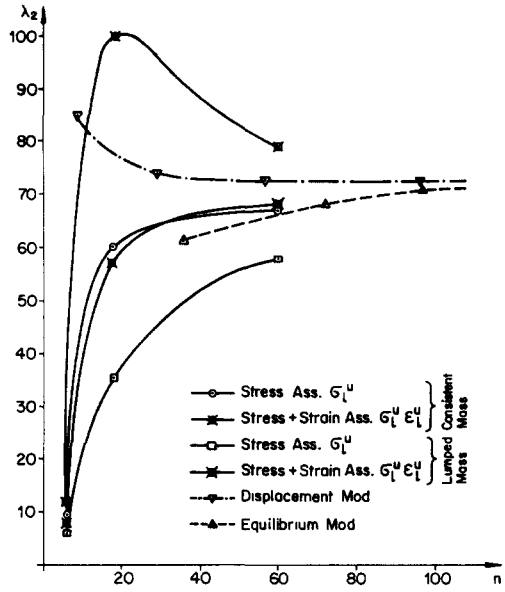

Fig. 3. Second lowest eigenvalue value λ_2 vs number of equations.

number of equations. As the shear strain γ_{xy} is assumed constant (equation 18c) and not linear like ϵ_x and ϵ_y (equations 18a, b), the behavior of the element is thus directional. For a given nodal layout, the stiffness matrix depends on the position and orientation of the coordinate system in which it is formed. Convergence is still reached, as in the limit, only constant terms appear.

To establish the response of a strongly distorted element and to examine the directional behavior, rhombic elements are used to calculate the skew ($\alpha = 30°$) simply supported thin plate ($(h/l) = (1/100)$, Poisson's ratio $\nu = 0{\cdot}3$) of Fig. 4. Under an evenly distributed load, the bending moments are infinite in the obtuse corner, using Kirchhoff's theory. No exact solution exists; Morley's results, using a series expansion with coefficients determined by the least-square method, are precise[17, 18]. The following boundary conditions are enforced.

$$w = 0 \tag{26a}$$

$$\phi_s = 0. \tag{26b}$$

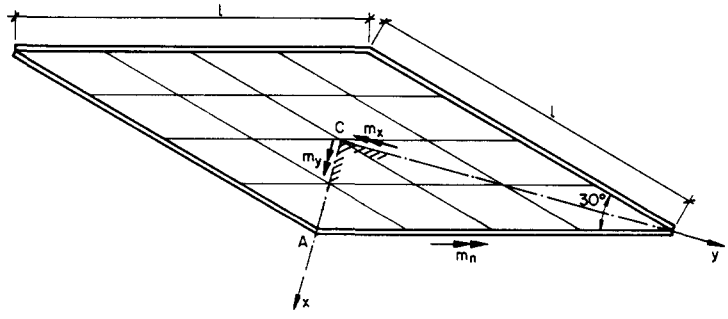

Fig. 4. Skew simply supported plate with 4 × 4 mesh.

Table 4. Results of hybrid models without and with independent strain expansion

			Analytical	Linear Moments Shear Def included 4x4 Mesh 75 Unknowns		Quadratic Moments Shear Def Excluded	
				Stress Ass σ_i^u	Stress+Strain Ass $\sigma_i^u \epsilon_i^u$	4x4 Mesh 75 Unknowns	16x16 Mesh 867 Unknowns
Vertical Displacement w (Centre)		$10^{-3} \cdot \frac{pl^4}{D}$	0 408	0 511	0 419	0 272	0 332
Principal Moments (Centre)	m_x	$10^{-2}\ pl^2$	1 91	1 85	2 21	1 57	1 70
	m_y	$10^{-2}\ pl^2$	1 08	1 26	0 89	0 44	0 81

A 4×4 mesh with 75 unknowns before enforcing the geometric boundary conditions is used for the models σ_i^u and $\sigma_i^u\ \epsilon_i^u$. The stress expansion is not modified on the simply supported boundary.

In Table 4, the vertical displacement w and the two principal moments m_x, m_y at the centre of the plate are listed. The stress couples are averaged proportionally to the angles of the elements meeting at the centre. For comparison, the results of an analysis with the same 4×4 mesh and with a very fine subdivision are listed, using hybrid stress models of rhomboid shape, based on a quadratic moment expansion and on cubic displacements and on linear rotations on the inter-element boundary. w and m_y of the model $\sigma_i^u \epsilon_i^u$ with a 4×4 mesh are more accurate than the corresponding values of the 16×16 mesh of the other hybrid stress model, which have been taken from Ref. [19].

In Fig. 5 the principal moment m_x from the Centre C to the obtuse Corner A of the plate is plotted. Considering the coarseness of the mesh (only 2 elements from C to A), the two models represent the singularity itself quite satisfactorily.

To study the directionality further, the simply supported rhomboid plate is analyzed with a 2×2, 4×4 and 8×8 mesh for a concentrated load applied in the centre of the plate. For this case,

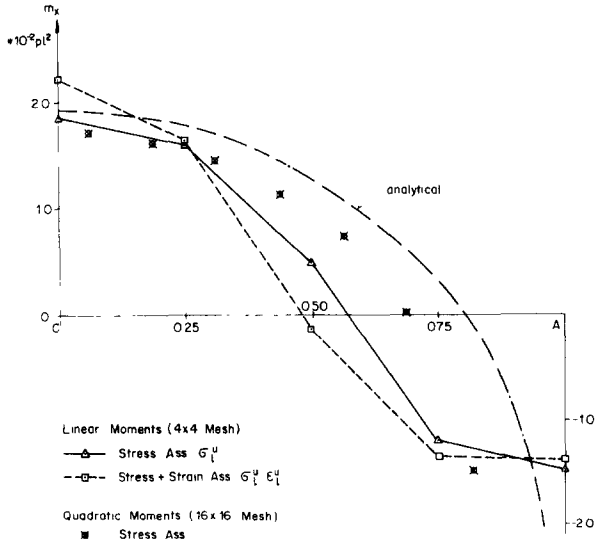

Fig. 5. Principal moment m_x from centre C to obtuse corner A of plate.

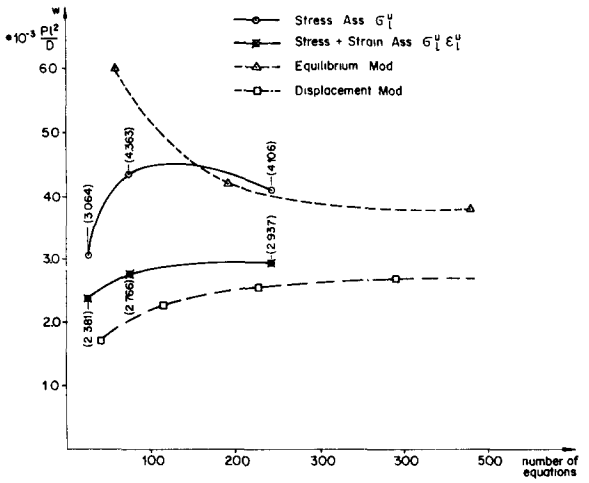

Fig. 6. Vertical displacement w under concentrated load P.

the tangential rotation ϕ_s is regarded as free; the geometric boundary condition consists of equation (26a) only. For comparison, the results of Sander[20] are used, who calculated the same plate, but with the geometric boundary conditions of equations (26a, b) using the displacement model of Fraeijs de Veubeke[15] and the triangular equilibrium model of Fraeijs de Veubeke *et al.*[16]. In Fig. 6 the vertical displacement w under the concentrated load, which is equal to the energy, is plotted vs the number of equations before enforcing geometric boundary conditions. The directional behavior decreases strongly as a finer mesh is chosen. The difference in the vertical displacement, which should be the same due to symmetry, is about 10 per cent for the 4×4 mesh and only 1 per cent for the 8×8 mesh.

Acknowledgements—The author wishes to express his gratitude to Professor B. Thürlimann for his guidance and support in the preparation of the Ph.D. Thesis[4] and to Professor W. Schumann for serving on the thesis committee, both of the Swiss Federal Institute of Technology, Zurich. In addition, particular thanks are due to Professor T. H. H. Pian of the Massachusetts Institute of Technology for his interest in the work of the author over the years.

REFERENCES

1. B. Fraeijs de Veubeke, Displacement and equilibrium models in the finite element method. *Stress Analysis* 145, Wiley, New York (1965).
2. T. H. H. Pian, Derivation of element stiffness matrices by assumed stress distributions. *AIAA-Journal*, **2**, 1333 (1964).
3. T. H. H. Pian and P. Tong, Basis of finite element methods for solid continua. *Intern. J. Numer. Meth. Engng*, **1**, 3 (1969).
4. J. P. Wolf, Generalized stress models for finite-element analysis, Ph.D. Thesis, Swiss Federal Institute of Technology (ETH), Zurich, Switzerland (Feb. 1974), also published as Report No. 52 of the Institute of Structural Engineering (Professor Dr. B. Thürlimann) (1974). Distributor: Birkhäuser, Basel, Switzerland. (ISBN-No. 3-7643-0745-5).
5. K. Washizu, *Variational Methods in Elasticity and Plasticity*. Pergamon Press, Oxford (1968).
6. J. P. Wolf, Generalized hybrid stress finite-element models. *AIAA-Journal*, **11**, 386 (1973).
7. T. H. H. Pian, Finite element methods by variational principles with relaxed continuity requirement. *Proc. Intern. Conf. Varia. Meth. Engng*, Southampton, (Sept. 1972).
8. K. Willam, Finite element analysis of cellular structures. Doctoral Dissertation, University of California, Berkeley, Dept. of Civil Engineering, (Dec. 1969).
9. S. T. Mau, P. Tong and T. H. H. Pian, Finite element solutions for laminated thick plates. *J. Comp. Mat.*, **6**, 304 (1972).
10. S. T. Mau and E. A. Witmer, Static vibration and thermal stress analysis of laminated plates and shells by the hybrid-stress finite element method, with transverse shear deformation effects included. *M.I.T., Aeroelastic and Structures Res. Lab.* TR 169-2, (Oct. 1972).

11. T. H. H. Pian and S. T. Mau, Some Recent Studies in Assumed Stress Hybrid Model. Second Japan-U.S. Seminar on Matrix Methods of Structural Analysis, Berkely (Aug. 1972), *Advances in Computational Methods in Structural Mechanics and Design*, University of Alabama Press, Huntsville (1972).
12. S. Timoshenko and Woinowsky-Krieger, *Theory of Plates and Shells*. McGraw–Hill, New York (1959).
13. E. Reissner, Small bending and stretching of sandwich type shells. *NACA-TN-Rep.* 975 (1950).
14. M. Geradin, Computational Efficiency of equilibrium models in eigenvalue analysis, Proc. IUTAM-Symp. High Speed Computing of Elastic Structures. Liège, (August 1970), Vol. 61 (1971).
15. B. Fraeijs de Veubeke, A conforming finite element for plate bending. *Int. J. Solids Struct.*, **4**, 95 (1968).
16. B. Fraeijs de Veubeke and G. Sander, An equilibrium model for plate bending. *Int. J. Solids Struct.*, **4**, 447 (1968).
17. L. S. D. Morley, Bending of a simply supported rhombic plate under uniform normal loading. *Q. J. Mec. Appl. Math.*, **15** (1962).
18. L. S. D. Morley, *Skew Plates and Structures*. Pergamon Press, Oxford (1963).
19. J. P. Wolf, Systematic enforcement of stress boundary conditions in the assumed stress hybrid model based on the deformation method. *Proc. 1st Int. Conf. on Structural Mechan. in Reactor Technol.*, Berlin, Sept. 1971, Part M 6, Paper 10.
20. G. Sander, Application de la méthode des eléments finis à la flexion des plaques. Ph.D. Thesis, University of Liège, Faculty of Applied Sciences, No. 15 (1969).